DOI: 10.1534/genetics.108.089094

A Misexpression Screen to Identify Regulators of Drosophila Larval Hemocyte Development

Martin Stofanko, So Yeon Kwon and Paul Badenhorst[1]

Institute of Biomedical Research, University of Birmingham, Edgbaston B15 2TT, United Kingdom

Manuscript received March 14, 2008
Accepted for publication July 14, 2008

ABSTRACT

In Drosophila, defense against foreign pathogens is mediated by an effective innate immune system, the cellular arm of which is composed of circulating hemocytes that engulf bacteria and encapsulate larger foreign particles. Three hemocyte types occur: plasmatocytes, crystal cells, and lamellocytes. The most abundant larval hemocyte type is the plasmatocyte, which is responsible for phagocytosis and is present either in circulation or in adherent sessile domains under the larval cuticle. The mechanisms controlling differentiation of plasmatocytes and their migration toward these sessile compartments are unclear. To address these questions we have conducted a misexpression screen using the plasmatocyte-expressed GAL4 driver *Peroxidasin-GAL4* (*Pxn-GAL4*) and existing enhancer-promoter (EP) and EP yellow (EY) transposon libraries to systematically misexpress ~20% of Drosophila genes in larval hemocytes. The *Pxn-GAL4* strain also contains a *UAS-GFP* reporter enabling hemocyte phenotypes to be visualized in the semitransparent larvae. Among 3412 insertions screened we uncovered 101 candidate hemocyte regulators. Some of these are known to control hemocyte development, but the majority either have no characterized function or are proteins of known function not previously implicated in hemocyte development. We have further analyzed three candidate genes for changes in hemocyte morphology, cell–cell adhesion properties, phagocytosis activity, and melanotic tumor formation.

IN Drosophila, defense against foreign pathogens is mediated by the innate immune system, which is composed of both a humoral and cellular arm. Humoral responses include the rapid melanization and coagulation reactions that accompany wound healing and the production of antimicrobial peptides, principally by the larval fat body. In larvae, the cellular arm consists of circulating hemocytes that engulf bacteria and apoptotic cells and can encapsulate larger foreign particles. Three hemocyte cell types occur (reviewed in Lanot *et al.* 2001; Evans *et al.* 2003; Meister and Lagueux 2003). The most abundant is the plasmatocyte, which accounts for 95% of circulating hemocytes. Plasmatocytes are professional macrophages that can remove foreign material by phagocytosis and typically contain residual bodies or phagosomes containing lysosomal enzymes, reactive forms of oxygen, or nitric oxide (Jones *et al.* 1999). Less abundant are crystal cells (~5% of hemocytes), which are characterized by large crystalline inclusions of prophenoloxidases (Fujimoto *et al.* 1995) and are involved in melanin synthesis during pathogen encapsulation (Soderhall and Cerenius 1998) and wound healing (Lai-Fook 1966). The third hemocyte type is the lamellocyte. These large flattened cells are rarely found in the larval hemolymph in the absence of immune challenge. Lamellocytes encapsulate foreign bodies and are responsible for the formation of melanotic tumors (Luo *et al.* 1995).

Two waves of hematopoiesis occur. The first occurs during embryonic development when a population of hemocytes arises from the head mesoderm (reviewed in Tepass *et al.* 1994; Ramet *et al.* 2002). These hemocytes eventually populate the whole embryo. Prior to larval hatching, hemocytes are targeted to and concentrate at sites of cell death and phagocytose apoptotic cells (Abrams *et al.* 1993; Tepass *et al.* 1994). After larval hatching, hemocytes of embryonic origin persist and replicate in the larval hemolymph. At the same time, a second wave of hematopoiesis occurs in the larval lymph gland (Lanot *et al.* 2001; Holz *et al.* 2003; Jung *et al.* 2005). These hemocytes are liberated at metamorphosis and populate the pupa and adult fly (Holz *et al.* 2003). A number of transcription factors have been identified to control hemocyte development. All hemocytes express the GATA factor Serpent (Srp) (Rehorn *et al.* 1996; Lebestky *et al.* 2000), which is required for hemocyte determination and maturation. Differentiation of plasmatocytes requires expression of Glial cells missing (Gcm) (Bernardoni *et al.* 1997; Alfonso and Jones 2002). In turn, the transcription factors Lozenge (Bataille *et al.* 2005) and Collier (Crozatier *et al.* 2004) are required for proper crystal cell and lamellocyte development, respectively.

[1]*Corresponding author:* Institute of Biomedical Research, University of Birmingham, Edgbaston B15 2TT, United Kingdom.
E-mail: p.w.badenhorst@bham.ac.uk

Drosophila larvae have an open circulatory system. Circulation of the hemolymph (blood) is mediated by contractions of the dorsal vessel and by peristaltic movements of the body. There are ~5000 hemocytes in a mature third instar larva (Lanot *et al.* 2001). About two-thirds of these freely circulate in the hemocoel, but the remainder attach to the inner surface of the integument (Lanot *et al.* 2001). These sessile cells form segmentally repeated patches or "islets" of hemocytes and can also be found attached to the posterior of the larva. The sessile hemocyte compartments are in direct contact with the cuticle and contain plasmatocytes and crystal cells (Lanot *et al.* 2001).

Migration of hemocytes in the embryo is regulated by two mechanisms: chemotactic response to wounding and migration in response to signals from the platelet-derived growth factor/vascular endothelial growth factor (PDGF/VEGF) ligands Pvf2 and Pvf3 (Wood *et al.* 2006). However, the mechanisms controlling hemocyte adhesion and targeting to sessile islets in the larvae are not completely understood. It is known that Rac1 activation leads to release of cells from these domains (Williams *et al.* 2006). This release requires the activity of the Drosophila Jun N-terminal kinase Basket (Bsk) (Williams *et al.* 2006). In addition, sessile hemocyte compartments are disrupted at commencement of pupariation, suggesting that ecdysone signaling can modify their adhesive properties.

In an effort to understand the mechanisms that control larval hemocyte migration and differentiation, we have conducted a misexpression screen using the GAL4-UAS system (Brand and Perrimon 1993). We have used a hemocyte-specific GAL4 driver (*Peroxidasin-GAL4*) and a library of enhancer-promoter (EP) or EP yellow (EY) transposon insertion lines (Rorth 1996; Bellen *et al.* 2004) to misexpress ~20% of Drosophila genes in larval hemocytes. The *Pxn-GAL4* driver directs expression in plasmatocytes and crystal cells and also contains a *UAS-GFP* transgene that allows visualization of hemocytes in third instar larvae, which are semitransparent. Here we report the results of this screen. Among the 3412 insertions screened we identified 101 candidate genes that affect hemocyte development and migration. Detailed characterization of selected candidate genes is presented.

MATERIALS AND METHODS

Fly strains and genetic crosses: The w^{1118}*; Pxn-GAL4, UAS-GFP* driver used is as described in Stramer *et al.* (2005) and was a gift of M. Galko. The following UAS lines were used: *UAS-nejire* (Kumar *et al.* 2004) and *UAS-Kruppel* (Carrera *et al.* 1998). hop^{Tum-l} is described in Luo *et al.* (2005). *lozenge-lacZ* (Bataille *et al.* 2005) was a gift of L. Waltzer. *Lsp2-GAL4* was obtained from the Bloomington Drosophila Stock Center. The gain-of-function screen was performed with 567 *P{EP}* (EP) (Rorth 1996) and 2845 *P{EPgy2}* (EY) (Bellen *et al.* 2004) transposon insertion lines obtained from the Szeged and Bloomington Drosophila Stock Centers, respectively. For each cross, 5–10 virgin females of the w^{1118}*; Pxn-GAL4, UAS-GFP* driver line were independently crossed to 5 males of each EP and EY strain. For X chromosomal EP and EY insertions that are male sterile, the cross was performed using 5–10 virgin EP/EY females and 5 males of the w^{1118}*; Pxn-GAL4, UAS-GFP* driver line. Progeny larvae were staged using the blue gut method (Maroni and Stamey 1983) and 5–10 wandering third instar larvae from each cross were scored for defects in hemocyte development and distribution according to the parameters shown in Table 1. Hemocytes were visualized by GFP expression using an Olympus SZX12 stereomicroscope with GFP filter set. Candidate EP and EY lines that showed disrupted hemocyte development were retested to confirm that hemocyte phenotypes were reproducible. Lines that passed retest were selected for further study. For each positive line, other EP and EY lines that contained transposon insertions in the vicinity of the positive insertion were tested for similar overexpression phenotypes. Typically, these were insertions within the same gene and/or insertions located up to 10 kb upstream/downstream from the original positive insertion. All overexpression phenotypes were recorded and listed in supplemental Table 1.

TABLE 1

Scoring criteria used in the gain-of-function screen

Criterion	Scoring system
Hemocytes present	Y/N
Total hemocyte number under the cuticle	↑/↓
Total hemocyte number in circulation	↑/↓
Disrupted dorsal sessile compartment	1 (disrupted)–5 (wild type)
Inappropriate targeting of hemocytes	Y/N
Accumulation along the dorsal vessel	Y/N
Hemocytes spread throughout the cuticle	Y/N
Lymph gland size	↑/↓
Hemocyte shape changes	N/A

Immunohistochemistry: Circulating hemocytes were isolated from 10 wandering third instar larvae, staged as above. Larvae were ripped on ice in 200 μl of HyQ CCM3 culture medium (HyClone) containing protease inhibitors (Complete, Boehringer). Hemocytes were pelleted by centrifugation at 260 g for 10 min at 4°, the cells resuspended in 50 μl of HyQ CCM3 culture medium with protease inhibitors, and transferred to individual wells on a Multispot slide (PH-001; C. A. Hendley). Slides were incubated at room temperature for 30 min in a humid chamber to allow cells to attach to the slides and then fixed in 3.7% paraformaldehyde (Sigma) for 10 min. After fixation, slides were washed in phosphate-buffered saline (PBS) containing 0.1% Saponin (Sigma) for 10 min and then blocked overnight at 4° in blocking buffer (PBS containing 0.1% Saponin and 1% FCS). Primary antibody incubations were performed for 1 hr at room temperature in blocking buffer. All subsequent steps were performed in PBS containing 0.1% Saponin. Slides were washed three times for 10 min, followed by secondary antibody incubation for 30 min. Washes were repeated and the slides were mounted in Vectashield mounting media with DAPI (Vector Laboratories). Samples were observed using a Zeiss Axiovert 100M confocal microscope.

To prepare sessile hemocytes, individual larvae were cut to remove circulating hemocytes. Portions of cuticle that contained adherent hemocyte sessile patches were transferred to multispot slides in HyQ CCM3 containing protease inhibitors.

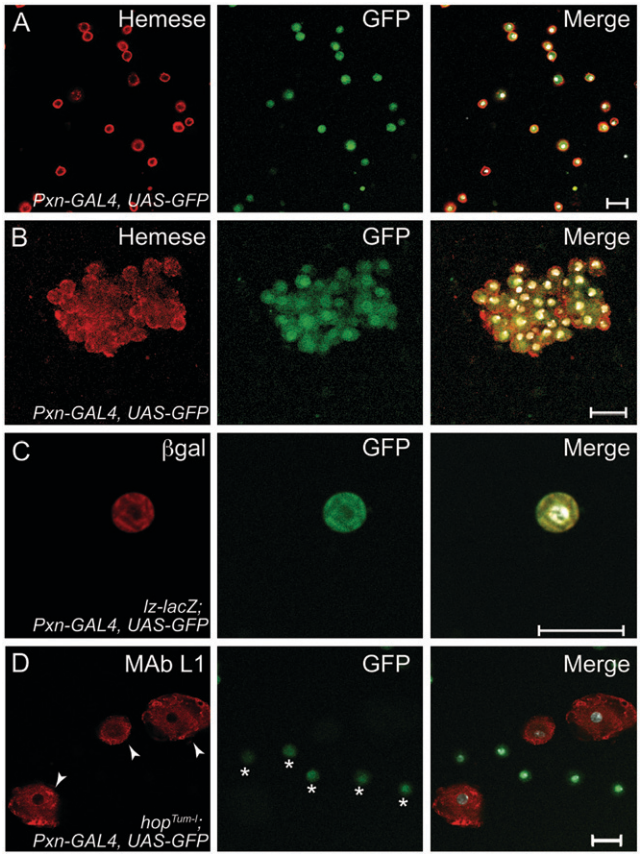

Figure 1.—Hemocyte expression of the *Pxn-GAL4* driver. (A) Circulating and (B) sessile hemocytes were isolated from wandering-stage *Pxn-GAL4, UAS-GFP* larvae and stained with antibodies against GFP (green) and the pan-hemocyte marker Hemese (red). (C) *Pxn-GAL4* directed expression of GFP (green) overlaps expression of the crystal cell marker *lozenge-lacZ* (*lz-lacZ*) (red). (D) Lamellocyte overproduction was triggered by introducing one copy of the $hop^{Tum\text{-}l}$ mutation into the *Pxn-GAL4, UAS-GFP* background. Lamellocytes (arrowheads, revealed by MAb L1b staining in red) do not express GFP (green). GFP-expressing plasmatocytes (asterisks) are not MAb L1b positive. Bar, 20 μm.

Sessile hemocytes were dislodged from the cuticle using a tungsten needle. The hemocytes were allowed to attach for 30 min and were fixed and processed for immunofluoresence as described above.

The following antibodies were used at the listed dilutions: polyclonal chicken anti-GFP antibody (1:400, Upstate Biotechnology), mouse MAb L1b (1:60, Sinenko *et al.* 2004), mouse MAb H2 anti-Hemese (1:50, Kurucz *et al.* 2003), mouse MAb CF.6G11 anti-Mys (1:20, Manseau *et al.* 1997), rabbit anti β-Int-υ (1:2000, Yee and Hynes 1993), rabbit anti-β-galactosidase (1:2000, Cappel), mouse MAb 40-1a anti-β-galactosidase (1:100). Secondary antibodies from Jackson Immunoresearch were: Cy3-conjugated anti-mouse IgG (H + L), FITC-conjugated anti-chicken IgY (H + L), and Cy3-conjugated anti-rabbit IgG (H + L), all used at 1:1000.

Live imaging microscopy: Wandering third instar w^{1118}*; Pxn-GAL4, UAS-GFP* larvae were washed and attached at their dorsal cuticle to transparent adhesive tape. The tape was then attached to a glass slide. Time-lapse images of GFP-expressing hemocytes were taken using a Zeiss Axiovert 100M microscope connected to a Hamamatsu C742-95 digital camera. Time-lapse images were analyzed using SimplePCI (Compix).

Molecular analysis: For selected lines we verified that the observed blood phenotypes were due to *Pxn-GAL4*-mediated overexpression of genes flanking the EP or EY insertion sites by analyzing gene expression using RT–PCR. Hemocytes were isolated from a total of 300 third instar larvae of each genotype. Larvae were bled into HyQ CCM3 culture media containing protease inhibitors and hemocytes pelleted by centrifugation at 260 g for 5 min at 4°. Hemocytes were washed twice with PBS. mRNA was isolated from hemocytes using a μMACS mRNA isolation kit (Miltenyi Biotec) according to the manufacturer's instructions. cDNA was generated by reverse transcription using Superscript II (Invitrogen) at 42°. PCR was performed for 25–32 cycles using gene-specific primers described in Table 2.

Phagocytosis assay: Phagocytosis was monitored by injection of India ink (black drawing ink; Stephens) into the hemocoel of third instar larvae. India ink was aliquoted into a 1.5 ml microfuge tube and centrifuged at maximum speed for 5 min to precipitate large particles. The supernatant was transferred to a drawn glass injection needle (TW100F-4; World Precision Instruments). Staged wandering third instar larvae were immobilized on double-sided tape (Scotch 665; 3M) attached to a glass slide. Larvae were injected with India ink using an Eppendorf Femtojet microinjector and Leitz Labovert inverted microscope with injection stand and needle holder (Leitz). Injections were made laterally through the larval cuticle into the body cavity. Larvae were incubated for 40 min at room temperature and hemocytes prepared for microscopy as described above.

RESULTS

Characterization of the *Pxn-GAL4* driver line: The *Peroxidasin-GAL4* (*Pxn-GAL4*) driver line expresses GAL4 in embryonic macrophages and has proven to be a useful tool for live imaging of macrophages during embryonic wound healing (Stramer *et al.* 2005). We reasoned that *Pxn-GAL4* would be a suitable GAL4 driver to be used in a gain-of-function genetic screen for regulators of larval hemocyte development. To confirm the suitability of *Pxn-GAL4*, we first established its expression profile in larval hemocytes. As shown in Figure 1A, we observed that *Pxn-GAL4* was able to drive *UAS-GFP* expression in larval hemocytes marked by the pan-hemocyte marker anti-Hemese. GFP expression was detected in 96% of circulating hemocytes of third instar larvae (data not shown). Expression was detected in both plasmatocytes (Figure 1A) and crystal cells (Figure 1C), but was not detected in mature lamellocytes (Figure 1D).

As Drosophila larval cuticles are transparent, the distribution of *Pxn-GAL4*-expressing cells in live animals could be examined by viewing expression of a *UAS-GFP* reporter. As shown in Figure 2, hemocyte expression of *Pxn-GAL4* could be detected in all larval instars. Expression was largely restricted to hemocytes although weak expression could be observed in the fat body of third instar larvae. From the second larval instar, GFP-expressing hemocytes could also be detected in the lymph gland, consistent with previous reports (Jung *et al.* 2005). Expression was noted in circulating hemocytes but two populations of adherent or sessile cells

TABLE 2

Primer pairs used for RT–PCR analysis

Gene	Primer name	Primer sequence (5′ to 3′)	Product length (bp)
CG32813	CG32813_5P	ACTCACAGGATGCCTTGGTC	167
	CG32813_3P	CTCCTGGGGATCCTGATTCT	
CG11448	CG11448_5P	CCGGCCAGTCTAAATCAAGG	163
	CG11448_3P	GAACGAGGATCGGACTGAGA	
CG15321	CG15321_5P	TGTGTCTGCTGCTGTTCGAC	180
	CG15321_3P	CCGCTTGACCAGTACCTCTT	
nejire	nej_5P	CCAGCACATCCTTGCCATAC	236
	nej_3P	GCTGCTGGTTCATCATGTGC	
buttonhead	btd_5P	GCCAGTTCATCCTCATCCTC	247
	btd_3P	GATAACTGGCCGCATACTCG	
Kruppel	kr_5P	ATGCTTGTTACCGCCAAACC	156
	kr_3P	GCATGTTTAGAGCGCCGATT	
Hemese	He_5P	TGGCACTCGGCGGAGCAGTTCACACTAAGT	491
	He_3P	GGTACTTTCAATGGGCTTGCATTGCTCTTT	
rp49	rp49_5P	TCTTGAGAACGCAGGCGACCGTTGGGGTTG	399
	rp49_3P	ATCCGCCACCAGTCGGATCGATATGCTAAG	

were also detected. From the first larval instar onwards, GFP-positive cells accumulated at the posterior of the larvae (arrowheads in Figure 2, A–C). From the second larval instar, GFP-expressing cells could also be observed in segmentally repeated patches along the dorsal midline on the inner surface of the integument (asterisks in Figure 2, B and C). These sessile hemocyte compartments bore superficial similarity to the hemocyte islets previously reported by Kitagawa and co-workers (Narita *et al.* 2004).

Antibody staining of these GFP-positive cells using the pan-hemocyte marker anti-Hemese, confirmed their identity as hemocytes (Figure 1B). Time-lapse live imaging of these sessile domains in *Pxn-Gal4, UAS-GFP* third instar larvae showed binding of circulating hemocytes to these regions (supplemental Figure 1), suggesting that they arise by recruitment of hemocytes out of circulation. During the course of live imaging of these sessile hemocyte patches, rearrangement of hemocytes within the compartment, and detachment of cells, was also observed (supplemental Figure 2), suggesting that they are dynamic. Indeed, shortly before pupariation, these sessile populations disappeared as the cells began to detach from the regions under the cuticle (data not shown).

Gain-of-function screen: Prior to embarking on a large gain-of-function screen we conducted a pilot screen to establish a baseline for screening criteria and the range of possible phenotypes. We selected a number of UAS lines that express genes previously shown to affect hemocyte development, as well as a number of random EP insertions in genes with no previously described hemocyte function. As a result, a set of nine criteria was established upon which to score gain-of-function hemocyte phenotypes (Table 1). These included changes in hemocyte number; disruption of dorsal sessile hemocyte compartments; inappropriate targeting of blood cells, including accumulation along the dorsal vessel and spreading of hemocytes through-

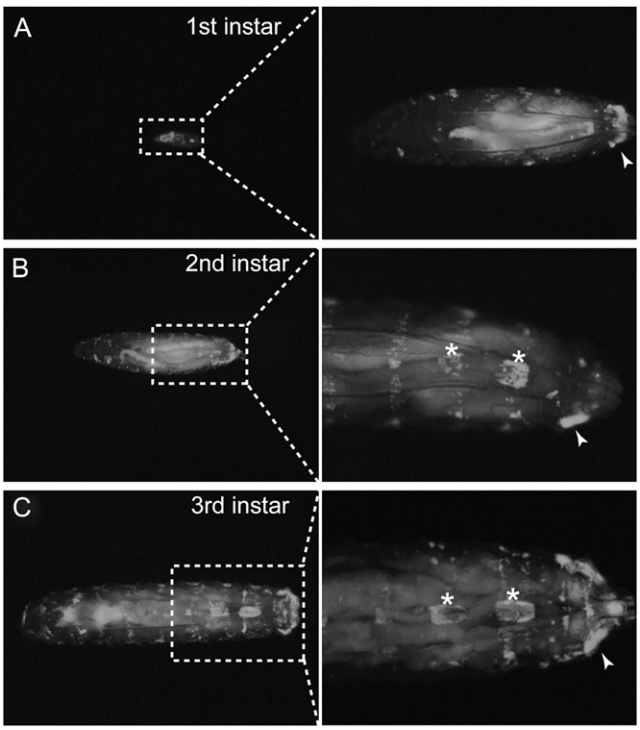

Figure 2.—Temporal profile of hemocyte accumulation. GFP-expressing hemocytes were visualized in *Pxn-GAL4, UAS-GFP* first, second, and third instar larvae. (A) In first instar larvae a sessile population of hemocytes forms at the posterior of the larva (arrowhead). (B) By the second instar larval stage, this posterior accumulation (arrowhead) is accompanied by the formation of distinct segmentally repeated dorsal patches or compartments (asterisks). (C) Third instar larvae show an increased number of hemocytes forming distinct dorsal sessile patches (asterisks) and accumulations at the tail region (arrowhead).

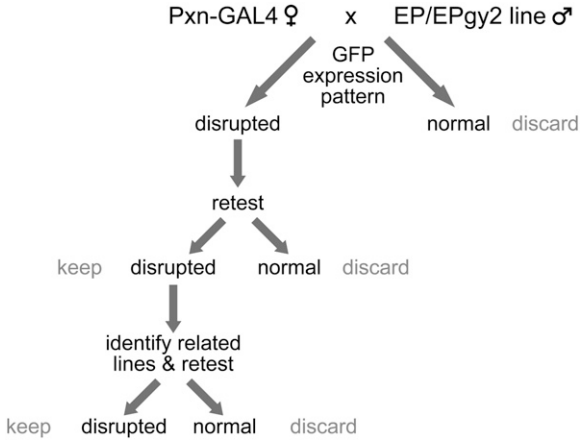

Figure 3.—Schematic of the screen. The *Pxn-GAL4, UAS-GFP* driver line was crossed to a set of EP and EY lines. The GFP blood expression pattern was recorded and the lines that show deviations from the parental pattern were retained (positives) and retested. For lines that pass the retest, EP/EY lines that contain insertions in the same gene or in close proximity were scored again for identical blood phenotypes.

out the cuticle; changes in lymph gland size; and changes in hemocyte shape.

The full screen was then performed as shown in Figure 3. We screened 567 EP and 2845 EY lines (3412 insertions in total) and recovered 108 insertions that disrupted hemocyte development according to at least one of the criteria in Table 1. These insertions corresponded to 101 gene loci as we had recovered a number of cases in which more than one selected EP/EY insertion had targeted the same locus. For example, *nejire* (*nej*) had been identified on the basis of overexpression phenotypes of both nej^{EP1149} and nej^{EP1179}. As shown in Figure 4, the most commonly observed phenotypes were disruption of dorsal sessile hemocyte compartments (58/108 insertions), changes in lymph gland size (54/108 insertions), changes in hemocyte number (37/108 insertions), accumulation of sessile hemocytes along the dorsal vessel (23/108 insertions), and spreading of sessile hemocytes throughout the cuticle (10/108 insertions). In numerous cases a combination of these phenotypes was observed. For example, $scab^{EY10270}$ (which overexpresses the α-integrin subunit αPS3) results in decreased circulating hemocyte number and lymph gland size, disrupts sessile dorsal sessile hemocyte compartments, and causes accumulation of hemocytes along the dorsal vessel. A full list of positive insertions and their phenotypes is provided in Table 3.

Disruption of dorsal sessile hemocyte compartments: We identified 58 lines representing 55 loci in which the dorsal sessile hemocyte patches were disrupted. This is the largest class of EP/EY insertions and includes genes that may regulate the adherent or migratory properties of hemocytes, for example, *scab* (*scb*, EY10270); *C3G* (EP1613), a Ras family guanine nucleotide exchange factor (Ishimaru *et al.* 1999); *RhoGEF2* (EY08391), which has been shown to direct cell shape changes (Barrett *et al.* 1997) and control invagination of mesodermal and endodermal primordia during gastrulation (Hacker and Perrimon 1998); and *tousled-like kinase* (*tlk*, EP1200), which has been identified as a regulator of Rho signaling (Gregory *et al.* 2007).

This class is also composed of a number of transcription factors and chromatin modifying enzymes. As shown in Figure 5B, overexpression of *Kruppel* (*Kr*) in

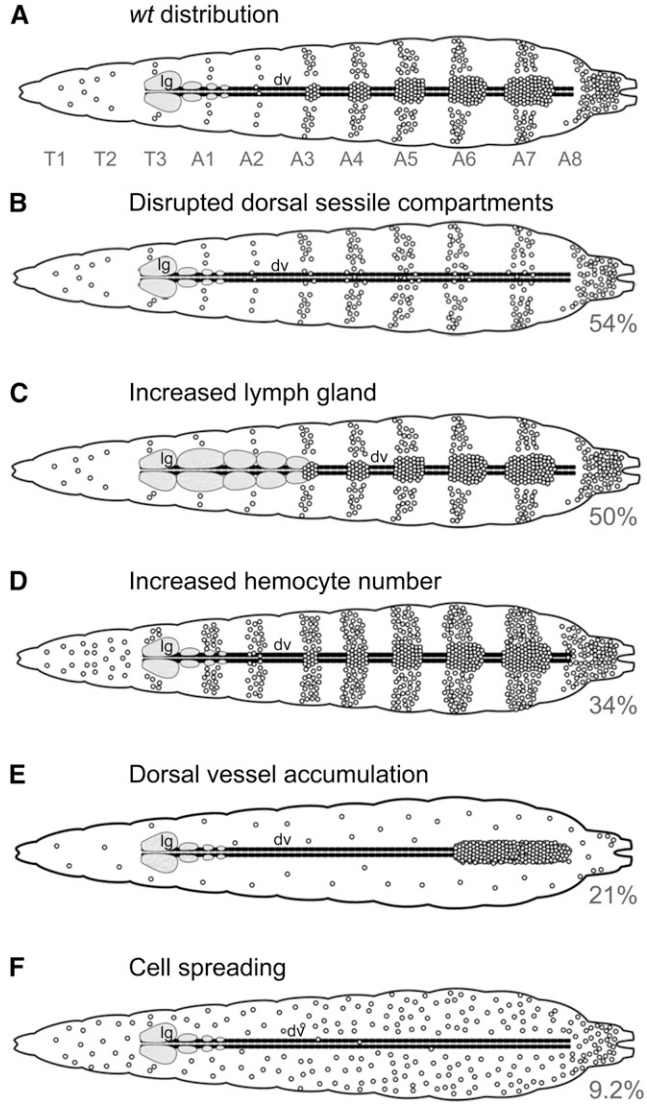

Figure 4.—Observed hemocyte phenotype classes. (A) Hemocyte distribution in wild-type third instar larvae. Principal overexpression phenotypes were (B) disruption of dorsal sessile hemocyte compartments; (C) increases in lymph gland size; (D) increases in hemocyte number; (E) relocalization of hemocytes to the dorsal vessel; and (F) spreading of hemocytes through the cuticle. Hemocytes are indicated as circles, lymph glands (lg) are shaded in the anterior of the larva, the dorsal vessel (dv) runs the length of the animal. Thoracic and abdominal segments are indicated (T1–A8).

TABLE 3

Genes identified in the gain-of-function screen

Gene	Transposon insertion	Chromosome	Hemocytes present	Hemocyte no. under cuticle	Hemocyte no. in circulation	Disrupted[a] dorsal sessile compartment	Inappropriate targeting of hemocytes	DV[b] accumulation	Hemocytes spread through cuticle	LG size[c]	Cell shape changes
ban	P{EPgy2}EY09041	3L	Y	Increased	Normal	5	N	Y	N	Increased	N
bbx	P{EPgy2}EY09604	X	Y	Decreased	Decreased	1	N	N	N	Normal	N
br	P{EP}EP1515	X	Y	Increased	Normal	5	Y	N	N	Normal	N
bru-3	P{EPgy2}EY08487	3L	Y	Increased	Increased	5	N	N	N	Increased	N
C3G	P{EP}EP1613	X	Y	Normal	Normal	3	Y	Y	N	Normal	N
cdc14	P{EPgy2}EY10303	2L	Y	Normal	Normal	5	N	Y	N	Increased	N
CG10584	P{EPgy2}EY00182	3L	Y	Normal	Normal	4	N	N	N	Normal	N
CG10585	P{EPgy2}EY00037	3L	Y	Decreased	Decreased	3	N	N	N	Normal	N
CG10962	P{EP}EP1640	X	Y	Increased	Increased	4	Y	N	Y	Increased	N
CG11008	P{EPgy2}EY15488	3L	Y	Normal	Normal	5	N	N	N	Increased	N
CG11134	P{EP}EP514	X	Y	Normal	Normal	3	Y	Y	N	Increased	N
CG11226	P{EPgy2}EY16243	3L	Y	Increased	Normal	5	Y	Y	N	Increased	N
CG11399	P{EPgy2}EY11352	3L	Y	Normal	Normal	4	N	N	N	Normal	N
CG12316	P{EPgy2}EY07889	3L	Y	Increased	Increased	5	Y	N	N	Normal	N
CG12367	P{EPgy2}EY10775	2R	Y	Normal	Normal	5	N	N	N	Increased	N
CG1265	P{EPgy2}EY01092	3L	Y	Normal	Normal	4	N	N	N	Increased	N
CG12701	P{EPgy2}EY00172	X	Y	Increased	Increased	0	Y	N	Y	Normal	N
CG13775	P{EPgy2}EY09811	2L	Y	Increased	Increased	5	N	N	N	Increased	N
CG14816	P{EPgy2}EY05994	X	Y	Increased	Decreased	4	N	N	N	Normal	N
CG15083	P{EPgy2}EY00232	2R	Y	Increased	Normal	5	N	N	N	Normal	N
CG15771	P{EP}EP1405	X	Y	Normal	Normal	3	N	N	N	Increased	N
CG16854	P{EPgy2}EY09123	2L	Y	Increased	Increased	3	N	N	Y	Normal	N
CG18600	P{EPgy2}EY00186	3R	Y	Decreased	Normal	4	N	N	N	Normal	N
CG18854	P{EPgy2}EY00141	2L	Y	Normal	Normal	5	N	N	N	Normal	N
CG1888	P{EPgy2}EY14750	2R	Y	Normal	Normal	5	N	N	N	Increased	N
CG1888	P{EP}EP699	2R	Y	Normal	Normal	2	Y	N	N	Normal	N
CG2034	P{EPgy2}EY08817	3L	Y	Increased	Increased	5	Y	Y	Y	Normal	N
CG2249	P{EPgy2}EY11713	2R	Y	Increased	Normal	5	N	N	N	Increased	N
CG2608	P{EPgy2}EY00214a	2L	Y	Normal	Normal	5	N	N	N	Increased	N
CG31044	P{EPgy2}EY03350	3R	Y	Normal	Normal	2	N	N	N	Decreased	N
CG32165	P{EPgy2}EY14634	3L	Y	Normal	Normal	5	N	N	N	Increased	N
CG32556	P{EPgy2}EY11178	X	Y	Decreased	Decreased	2	N	N	N	Increased	N
CG32813	P{EPgy2}EY07727	X	Y	Decreased	Decreased	2	Y	Y	N	Increased	N
CG32813	P{EPgy2}EY14694	X	Y	Decreased	Decreased	3	Y	Y	N	Normal	N
CG33182	P{EPgy2}EY10737	2R	Y	Increased	Increased	5	N	N	N	Increased	N
CG3363	P{EPgy2}EY08136	2R	Y	Normal	Normal	5	N	N	N	Increased	N
CG3368	P{EP}EP752	3R	Y	Normal	Normal	5	N	N	N	Increased	N
CG3624	P{EPgy2}EY03617	2R	Y	Decreased	Decreased	3	N	N	N	Normal	Y

(*continued*)

TABLE 3

(Continued)

Gene	Transposon insertion	Chromosome	Hemocytes present	Hemocyte no. under cuticle	Hemocyte no. in circulation	Disrupted[a] dorsal sessile compartment	Inappropriate targeting of hemocytes	DV[b] accumulation	Hemocytes spread through cuticle	LG size[c]	Cell shape changes
CG3654	P{EPgy2}EY00142	3L	Y	Decreased	Normal	3	N	N	N	Increased	N
CG4807	P{EPgy2}EY09709	2L	Y	Increased	Increased	0	Y	Y	Y	Increased	N
CG4857	P{EPgy2}EY14284	X	Y	Increased	Increased	4	Y	N	N	Normal	N
CG4857	P{EPgy2}EY12989	X	Y	Normal	Normal	2	Y	N	N	Normal	N
CG4928	P{EP}EP1341	X	Y	Decreased	Decreased	3	Y	Y	Y	Normal	N
CG5009	P{EPgy2}EY10858	2R	Y	Normal	Normal	5	N	N	N	Increased	N
CG5104	P{EPgy2}EY04231	3L	Y	Decreased	Normal	3	N	N	N	Normal	N
CG5360	P{EPgy2}EY01258	2R	Y	Decreased	Decreased	4	N	N	N	Normal	N
CG5555	P{EPgy2}EY00181	3R	Y	Normal	Normal	2	N	Y	N	Increased	N
CG5577	P{EPgy2}EY08509	3L	Y	Normal	Normal	5	N	N	N	Increased	N
CG5720	P{EPgy2}EY08422	3R	Y	Decreased	Decreased	2	N	N	N	Normal	N
CG5899	P{EP}EP701	2L	Y	Increased	Increased	5	N	N	N	Normal	N
CG5946	P{EPgy2}EY00183	3L	Y	Normal	Normal	5	N	N	N	Increased	N
CG6114	P{EPgy2}EY08774	3L	Y	Decreased	Decreased	2	N	N	N	Increased	N
CG6448	P{EPgy2}EY15308	2L	Y	Increased	Normal	5	N	N	N	Increased	N
CG6770	\P{EPgy2}EY11946	2L	Y	Decreased	Decreased	2	N	N	N	Normal	N
CG7182	P{EPgy2}EY08303	3L	Y	Normal	Normal	5	N	Y	N	Increased	N
CG7888	P{EPgy2}EY02590	3L	Y	Normal	Normal	5	N	N	N	Increased	N
CG8062	P{EP}EP1300	X	Y	Normal	Decreased	5	N	N	N	Increased	N
CG9243	P{EPgy2}EY11898	2L	Y	Normal	Normal	4	N	N	N	Increased	N
chn	P{EPgy2}EY06007	2R	Y	Decreased	Decreased	0	N	N	N	Normal	N
dan	P{EPgy2}EY11735	3R	Y	Decreased	Decreased	2	N	N	N	Normal	N
Dip2	P{EPgy2}EY12268	3R	Y	Increased	Increased	5	Y	N	N	Normal	N
dob	P{EPgy2}EY05880	X	Y	Increased	Increased	5	N	N	N	Normal	N
eg	P{EPgy2}EY00149	3L	Y	Increased	Normal	5	N	N	N	Increased	N
esg	P{EP}EP684	2L	Y	Increased	Increased	3	Y	N	Y	Normal	N
esg	P{EPgy2}EY10592	2L	Y	Normal	Normal	5	N	N	N	Increased	N
Fas1	P{EPgy2}EY06622	3R	Y	Increased	Increased	5	N	N	N	Increased	N
Gpdh	P{EPgy2}EY01534	2L	Y	Decreased	Normal	4	N	N	N	Normal	N
Gpdh	P{EP}EP466	2L	Y	Normal	Normal	5	N	Y	N	Increased	N
Gr93d	P{EPgy2}EY06917	3R	Y	Decreased	Decreased	1	N	N	N	Normal	N
grp	P{EPgy2}EY09600	2L	Y	Increased	Normal	5	N	N	N	Normal	N
GstS1	P{EP}EP641	2R	Y	Increased	Increased	5	Y	N	N	Normal	N
Hr38	P{EPgy2}EY14161	2L	Y	Normal	Normal	4	Y	Y	N	Normal	N
Hrb27C	P{EP}EP748	2L	Y	Normal	Normal	5	N	N	N	Normal	Y
InR	P{EPgy2}EY00681	3R	Y	Increased	Normal	4	Y	N	N	Normal	N
jigr1	P{EPgy2}EY06847	3R	Y	Increased	Increased	2	Y	N	Y	Increased	N
jim	P{EPgy2}EY14392	3L	Y	Increased	Increased	4	N	N	N	Increased	N

(*continued*)

TABLE 3

(Continued)

Gene	Transposon insertion	Chromosome	Hemocytes present	Hemocyte no. under cuticle	Hemocyte no. in circulation	Disrupted[a] dorsal sessile compartment	Inappropriate targeting of hemocytes	DV[b] accumulation	Hemocytes spread through cuticle	LG size[c]	Cell shape changes
kay	P{EPgy2}EY12710	3R	Y	Increased	Increased	5	N	N	N	Increased	N
Krn	P{EPgy2}EY11963	3L	Y	Normal	Normal	5	N	N	N	Increased	N
Kr	P{EPgy2}EY11357	2R	Y	Decreased	Decreased	0	N	N	N	Increased	Y
Mapmodulin	P{EPgy2}EY01282	2R	Y	Decreased	Normal	4	N	N	N	Increased	N
mir-9b	P{EPgy2}EY00118	2L	Y	Increased	Normal	5	N	N	N	Normal	N
Mov34	P{EP}EP687	2R	Y	Increased	Normal	5	Y	N	N	Normal	N
mts	P{EPgy2}EY00128	2L	Y	Normal	Normal	5	N	N	N	Increased	N
mub	P{EPgy2}EY11687	3L	Y	Normal	Normal	4	N	N	N	Normal	N
NA[d]	P{EPgy2}EY11817	3R	Y	Decreased	Decreased	2	N	N	N	Normal	N
NA	P{EPgy2}EY02882	3L	Y	Decreased	Normal	3	N	N	N	Normal	N
NA	P{EPgy2}EY14738a	2L	Y	Normal	Normal	2	Y	N	N	Increased	N
NA	P{EP}EP351	X	Y	Normal	Normal	3	N	N	N	Increased	N
NA	P{EP}EP1595	X	Y	Normal	Normal	4	N	Y	N	Increased	N
NA	P{EP}EP1351	X	Y	Normal	Normal	4	N	N	N	Increased	N
nej	P{EP}EP1149	X	Y	Decreased	Decreased	1	N	Y	N	Increased	N
nej	P{EP}EP1179	X	Y	Decreased	Decreased	2	N	Y	N	Normal	N
Nelf-E	P{EPgy2}EY07065	3L	Y	Increased	Increased	5	Y	N	Y	Increased	N
Ntf-2r	P{EPgy2}EY05573	2L	Y	Decreased	Decreased	3	N	N	N	Normal	N
Pbprp1	P{EPgy2}EY00168	3L	Y	Normal	Normal	5	N	N	N	Increased	N
rdo	P{EPgy2}EY15751	2L	Y	Normal	Normal	5	N	N	N	Increased	N
ras	P{EP}EP1519	X	Y	Normal	Normal	5	N	Y	N	Normal	N
RhoGEF2	P{EPgy2}EY08391	2R	Y	Increased	Normal	3	Y	N	N	Normal	N
RpI135	P{EPgy2}EY13368	2L	Y	Increased	Increased	5	Y	N	N	Increased	N
RpI135	P{EPgy2}EY12706	2L	Y	Increased	Normal	5	N	N	N	Increased	N
Rtnl1	P{EPgy2}EY06081	2L	Y	Decreased	Decreased	2	N	N	N	Normal	N
scb	P{EPgy2}EY10270	2R	Y	Decreased	Decreased	3	N	Y	N	Decreased	N
sced	P{EPgy2}EY09071	2R	Y	Decreased	Decreased	2	N	N	N	Normal	N
tlk	P{EP}EP1200	X	Y	Decreased	Decreased	1	N	Y	N	Normal	N
Tob	P{EPgy2}EY12182	X	Y	Decreased	Normal	2	Y	Y	N	Normal	N
tomosyn	P{EPgy2}EY00140	X	Y	Normal	Normal	5	N	N	N	Increased	N
Trp1	P{EP}EP663	2L	Y	Increased	Increased	5	Y	Y	Y	Normal	N
Vha16	P{EPgy2}EY00180	2R	Y	Increased	Increased	5	N	Y	N	Normal	N

[a] 5, normal; 1, most disrupted.
[b] DV, dorsal vessel.
[c] LG, lymph gland.
[d] NA, not annotated.

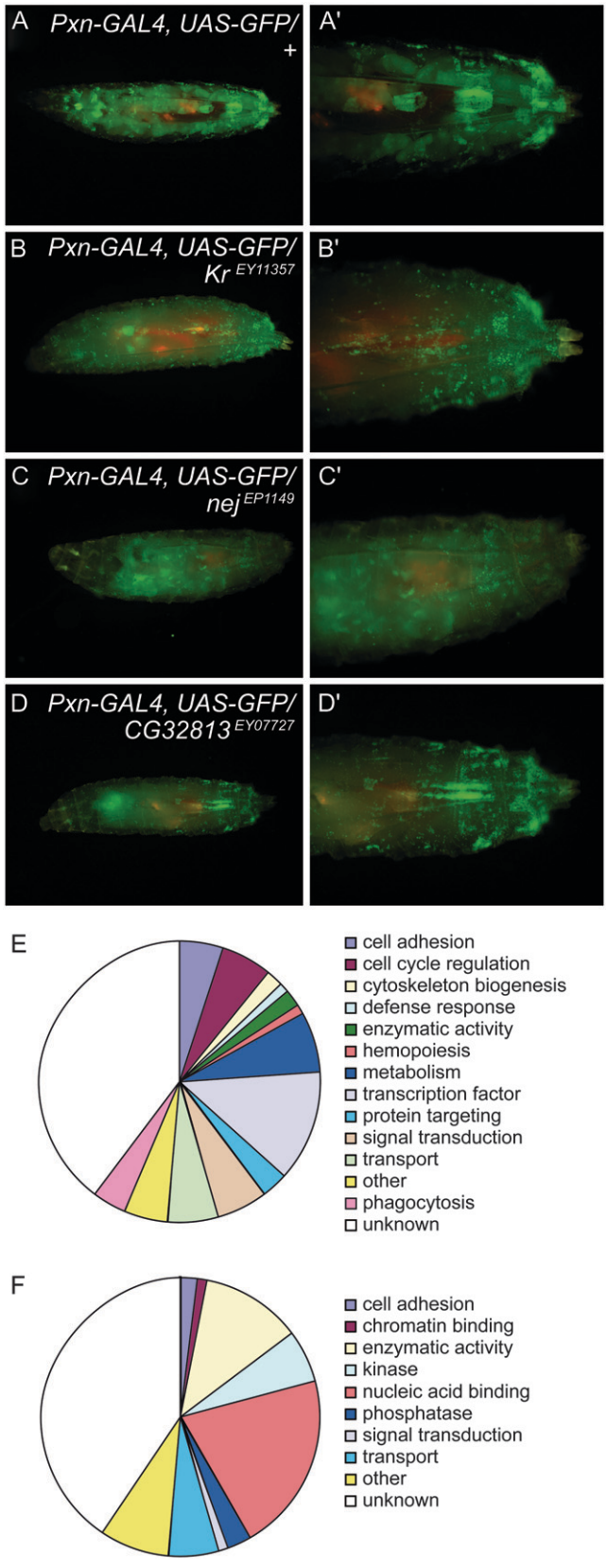

Figure 5.—Selected overexpression phenotypes and gene ontology classification of candidate genes. (A) Hemocyte distribution in control *Pxn-GAL4, UAS-GFP* third instar larvae. (A′) Detail of the posterior of the same larva showing the distinct dorsal sessile compartments. (B) *Pxn-GAL4* directed ectopic expression of *Kr* changes hemocyte distribution and morphology. (B′) Large flattened cells are observed. (C) Ectopic expression of *nej* results in generally weaker GFP expression in most hemocytes in both circulating and sessile populations apart from a few highly expressing cells. (D) Ectopic expression of *CG32813* results in inappropriate hemocyte targeting along the posterior of the dorsal vessel (enlarged detail shown in D′). GO classification of the 101 identified candidate genes according to (E) biological process, and (F) molecular function. GO annotations were obtained from FlyBase.

hemocytes using EY11357 disrupted sessile dorsal compartments and resulted in isolated large flattened cells (Figure 5B′). *Kr* is a segmentation gene, which is also known to regulate muscle identity (Ruiz-Gomez *et al.* 1997). Two insertions in the Drosophila CBP homolog *nejire* (EP1149 and EP1179) were also observed to disrupt sessile hemocyte domains as well as reduce circulating and sessile hemocyte numbers (Figure 5, C and C′). Other transcription regulators that displayed this phenotype included *escargot* (*esg*), which regulates cell adhesion and motility during tracheal branch fusion (Tanaka-Matakatsu *et al.* 1996); *charlatan* (*chn*), a zinc finger repressor of *Delta* and regulator of proneural gene expression (Escudero *et al.* 2005; Tsuda *et al.* 2006); and *distal antenna* (*dan*).

Disruption of the dorsal sessile hemocyte compartments was often accompanied by relocalization of hemocytes to ectopic locations. Two main classes of phenotype were observed: (i) hemocytes accumulated along the dorsal vessel and (ii) hemocytes were spread throughout the larval cuticle.

Hemocytes accumulate along the dorsal vessel: We identified 23 lines representing 21 loci in which sessile hemocytes were targeted to the dorsal vessel. One of the most striking examples was generated by overexpression of *CG32813* using EY07727 (Figure 5, D and D′). The functions of *CG32813* are unclear, but it is expected that this phenotype could be induced by changes in adherent or migratory properties of hemocytes. This is confirmed by other insertions that display the same phenotype. These included *raspberry* (EP1519), which has been implicated in the control of axon guidance (Long *et al.* 2006), and Rho signaling (Gregory *et al.* 2007), and as described previously, *scb*, *C3G*, and *tlk*.

Spreading of hemocytes throughout the cuticle: In 10 instances sessile hemocytes were observed to spread throughout the larval cuticle. This group comprised a number of known transcription factors such as *esg* or proteins that are predicted to function as transcription regulators such as the zinc finger protein CG12701 and CG2034, the Drosophila homolog of DERP6 (Yuan *et al.* 2006). An additional member of this class included *Nelf-E*, which encodes the RNA-binding subunit of NELF, a negative regulator of the RNA polymerase II transcription elongation (Yamaguchi *et al.* 1999). There is some evidence that regulation of transcript elongation by

NELF may be used to control cell fate determination in Drosophila (Wang *et al.* 2007).

Increased hemocyte number: We identified 37 lines representing 36 loci in which hemocyte number was increased. This class includes genes that have previously been linked to cell proliferation, for example, *bantam* (EY09041), a microRNA that controls proliferation and apoptosis (Brennecke *et al.* 2003); the Drosophila CHK1 homolog *grapes* (EY09600); the Drosophila *Insulin-like receptor* (EY00681), which can control cell size and number (Brogiolo *et al.* 2001); and *kayak* (EY12710), the Drosophila Fos homolog. This class also included a number of nucleic acid-binding and chromatin-modifying enzymes that have not previously been linked to cell proliferation or apoptosis, for example, *bruno-3* (EY08487), an RNA-binding protein that can bind to the EDEN translational repression sequence (Delaunay *et al.* 2004). Other genes of interest include the histone H3K9 demethylase *CG33182* (EY10737), the Drosophila SMARCAD1 chromatin remodeling enzyme *CG5899* (EP701), the transcriptional regulator *eagle* (EY00149), and the JAK/STAT pathway repressor *jim* (EY14392) (Mukherjee *et al.* 2006).

Increased lymph gland size: This was the second most commonly observed phenotype and included 54 insertions corresponding to 53 loci. Genes that resulted in increased hemocyte number were often included in this category, for example, *bantam*, *bruno-3*, *CG33182*, *eagle*, *kayak*, and *jim*. Additional genes that may control cell proliferation or survival that were identified included *cdc14* (EY10303), the EGF receptor ligand *Keren* (EY11963), and *CG11134* (EP514), the Drosophila homolog of the APIP inhibitor of cell death. In addition to the histone H3K9 demethylase *CG33182*, the Drosophila Jumonji homolog *CG3654* was also identified as a regulator of lymph gland size.

Functional classification of screen selected genes: Gene ontology (GO) classification of the 101 identified genes according to biological process and molecular function (validated by FlyBase) revealed that more than half of the genes identified in the screen had no previously described function. The next most abundant GO category was transcription factors (biological process, Figure 5E) or nucleic acid binding proteins (molecular function, Figure 5F). Examples included *Kr*, *esg*, *chn*, and *broad* (*br*), a primary responder to ecdysone signaling that is also required for proliferation and differentiation of lamellocytes and crystal cells (Sorrentino *et al.* 2002).

Another abundant class of genes included those involved in signal transduction. Examples included *C3G* and the Drosophila homolog of Transducer of ERBB2 (*Tob*). Tob proteins contain a conserved N-terminal BTG domain and were initially identified as negative regulators of cell proliferation, although have now been shown to participate in a number of signaling pathways (Jia and Meng 2007). The observed phenotype with decreased hemocyte number is consistent with a function in hemocyte proliferation. The gene *Hormone receptor-like in 38* (*Hr38*) appears to mediate an atypical Ecdysteroid signaling pathway (Baker and Zitron 1995). When overexpressed in blood cells using the EY14161 responder, sessile hemocyte patches are disrupted. It is known that the ecdysone signaling preceding pupariation disrupts sessile hemocyte patches.

Other categories of genes that were detected included regulators of cell adhesion, for example, *scb* and *Fasciclin 1*; cell cycle regulators, for example, *grapes* and *cdc14*; and genes controlling cytoskeleton dynamics. The latter were of particular interest given that identification of modifiers of hemocyte migration and adhesion was an objective of this screen. Examples included *RhoGEF2* which has been shown to direct cell shape changes (Barrett *et al.* 1997) and control invagination of mesodermal and endodermal primordia during gastrulation (Hacker and Perrimon 1998) and *microtubule star*.

Further analysis of selected EP/EY lines: On the basis of the phenotypes obtained, we selected three genes for further analysis: the segmentation gene *Kr*, the histone acetyltransferase *nej*, and the gene of unknown function *CG32813*. In an initial series of experiments we validated that the observed overexpression phenotypes obtained using EP/EY insertions in these genes were in fact due to overexpression of the tagged gene. A first simple test was to confirm that other EP/EY insertions that are inserted in a location and orientation to overexpress the same gene yielded an identical misexpression phenotype. Conversely, EP/EY lines that are inserted in the vicinity of the gene, but in an orientation that does not allow overexpression of the gene should not yield the same phenotype. An example is shown in Figure 6A where the EP insertions nej^{EP1149} and nej^{EP1179}, which are both predicted to overexpress *nej*, both generated the same overexpression phenotype. Conversely, nej^{EP950} and nej^{EP1410}, which are inserted in reverse orientation and should not overexpress *nej*, failed to give a phenotype when crossed to *Pxn-GAL4*.

Next we verified by RT–PCR that EP/EY lines selected in the screen did indeed overexpress the putative target gene. Hemocytes were isolated from third instar larvae of the appropriate genotypes, mRNA was purified, and the abundance of transcripts was determined using gene-specific primers. As shown in Figure 6, in all cases analyzed EP/EY insertions selected in the screen were able to drive significant overexpression of the designated target gene. Thus when crossed to *Pxn-GAL4* both nej^{EP1149} and nej^{EP1179} significantly increased expression of *nej* relative to the parental *Pxn-GAL4* control (Figure 6A). Similarly, $Kr^{EY11357}$ and $CG32813^{EY07727}$ also predominantly increased expression of their corresponding target genes (Figure 6, B and C).

Finally, phenotypes were confirmed using existing UAS lines, which express only the cDNA encoding the

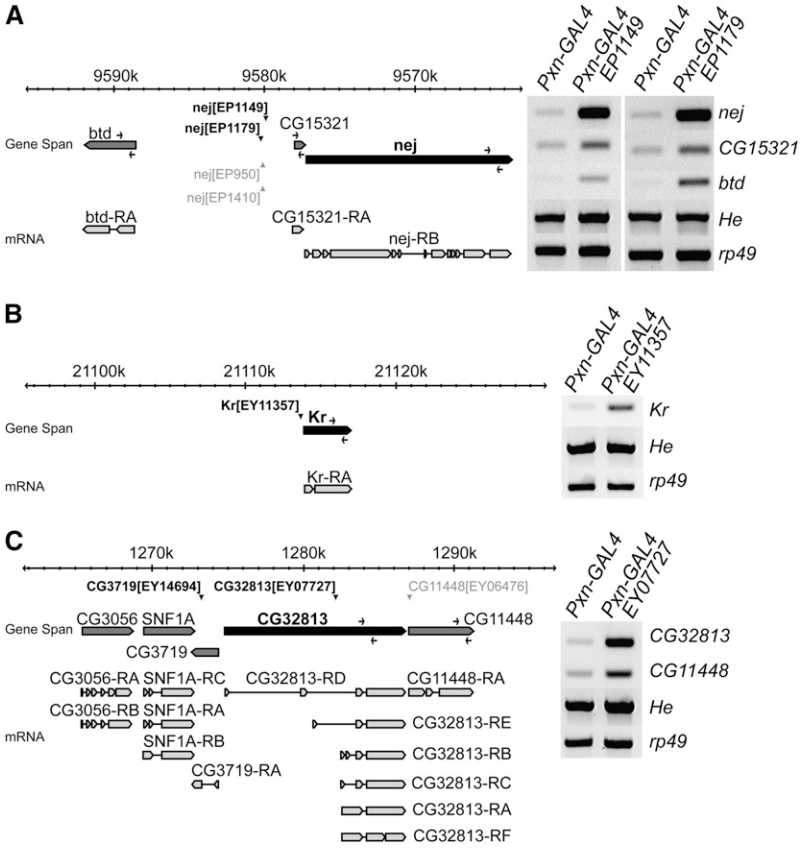

FIGURE 6.—Validation of selected EP/EY insertions. Expression of genes flanking EP/EY insertions identified in the screen was determined by RT–PCR. Insertions identified in the screen are indicated in boldface type while those that failed to give a hemocyte phenotype are shaded. (A) Two EP insertions in the *nejire* (*nej*) locus, *EP1149* and *EP1179* were selected as positives in the screen. RT–PCR on isolated hemocytes reveals that both *EP1149* and *EP1179* drive significant overexpression of *nej* but not of the flanking genes, *buttonhead* (*btd*) and *CG15321*. The EP insertions *EP950* and *EP1410* (shaded), which are inserted in an opposite orientation to *EP1149* and *EP1179* and are not predicted to overexpress *nej*, do not give a hemocyte overexpression phenotype. (B) RT–PCR confirms that the *EY11357* insertion drives overexpression of *Kr* when crossed to *Pxn-GAL4*. No other predicted genes occur within 10 kb upstream or downstream of *EY11357*. (C) Two EY insertions in the *CG32813* locus, *EY07727* and *EY14694*, were identified in the screen. RT–PCR indicates that *EY07727* drives overexpression of *CG32813* when crossed to *Pxn-GAL4*. *CG11448*, which flanks *CG32813*, shows slight increase in expression. However, the *EY06476* insertion, which is predicted to drive overexpression of *CG11448*, does not give a hemocyte overexpression phenotype. In A–C, *He* and *rp49* are used as loading controls and to assess mRNA purity.

gene of interest. Thus, phenotypes obtained after crossing nej^{EP1149} or *UAS-nej* (KUMAR *et al.* 2004) to *Pxn-GAL4* were identical (data not shown). Similarly, overexpression phenotypes obtained using $Kr^{EY11357}$ and *UAS-Kr* (CARRERA *et al.* 1998) were indistinguishable.

Hemocyte phenotypes of selected EP/EY lines: Next we determined the changes that occurred in hemocytes after overexpression of *Kr*, *nej*, or *CG32813* that could have accounted for the observed phenotypes. Hemocytes were isolated from wandering-stage third instar larvae and stained first with the pan-hemocyte marker anti-Hemese to reveal alterations in hemocyte morphology. As shown in Figure 7B, overexpression of *Kr* in hemocytes resulted in differentiation of many large hemocytes together with smaller hemocytes of irregular profile, unlike the parental *Pxn-GAL4/+* driver control in which a uniform population of round plasmatocytes was observed (Figure 7A). After overexpression of *nej* (Figure 7C) and *CG32813* (Figure 7D) most hemocytes appeared wild type, although a few larger cells could also be detected.

These larger cells appeared similar to lamellocytes, a hemocyte type that is rarely found in circulation. To establish if overexpression of *Kr*, *nej*, or *CG32813* led to the production of lamellocytes, isolated hemocytes were stained with the lamellocyte-specific antibody MAb L1b. As shown in Figure 7, E–H, overexpression of any of these proteins was able to trigger increased lamellocyte number. Counts of lamellocyte number as a proportion of total hemocyte number revealed that lamellocyte frequency increased from 0.5% in the parental *Pxn-GAL4/+* driver control to 9.5% after *Kr* overexpression, 5.5% after *nej* misexpression, and 3.8% after *CG32813* overexpression.

However, differentiation of the alternative lamellocyte cell type could only partially explain the changes in hemocyte distribution observed with these lines, as lamellocyte frequencies were still comparatively low. To ascertain, whether adhesive properties of hemocytes were changed, we examined expression of the Drosophila β-integrin subunit Myospheroid (Mys). Weak expression of Mys was detected in the parental *Pxn-GAL4/+* driver control (Figure 7M). In contrast, strong upregulation of Mys in hemocytes >15 μm was seen in all overexpression experiments (Figure 7, N–P). This suggested that adhesive properties of these cells had altered. Consistent with this, staining of filamentous actin (F-actin), using rhodamine-phalloidin, revealed changes in actin polymerization following overexpression of *Kr*, *nej*, and *CG32813*. Weak F-actin staining was detected in plasmatocytes of the parental *Pxn-GAL4/+* driver control (Figure 7I). However strong F-actin staining was detected in *Kr* (Figure 7J), *nej* (Figure 7K), and *CG32813* (Figure 7L) overexpressing hemocytes, suggesting that these hemocytes are actively polymerizing and depolymerizing their actin cytoskele-

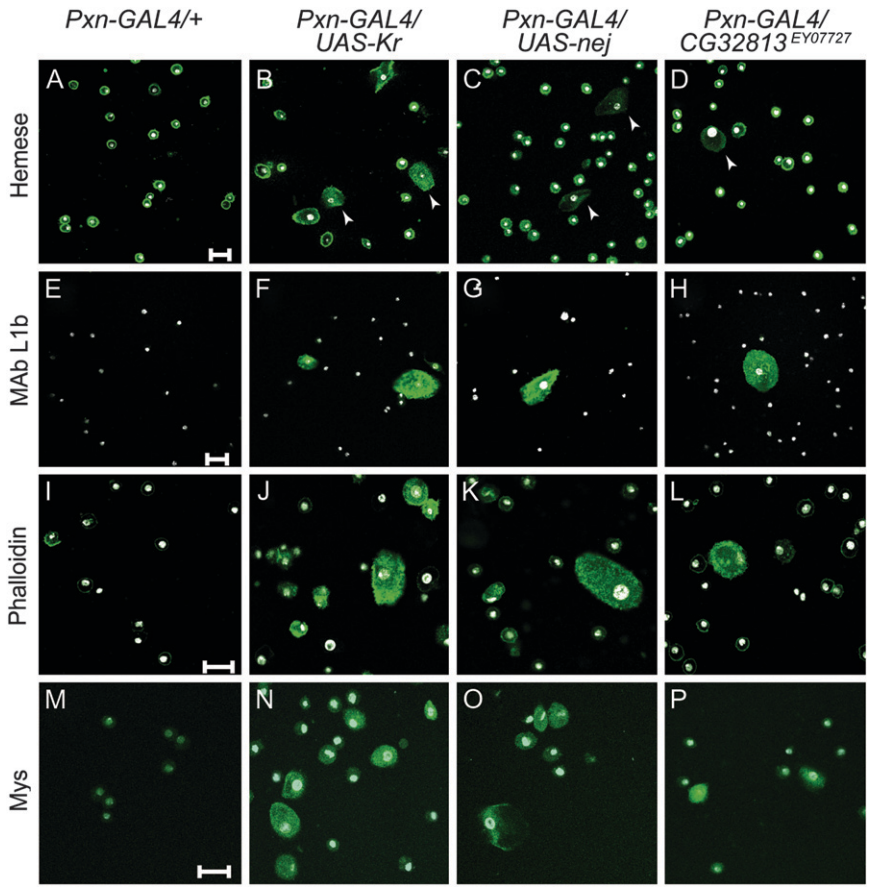

FIGURE 7.—Hemocyte phenotypes following *Pxn-GAL4* mediated overexpression of *Kr*, *nej*, and *CG32813*. (A–D) Hemocyte morphology was revealed using the pan-hemocyte marker anti-Hemese (MAb H2). In the parental *Pxn-GAL4* driver a uniform population of round plasmatocytes is detected. Overexpression of *nej*, *Kr*, or *CG32813* results in the appearance of lamellocytes (arrowheads) and some hemocytes with irregular profiles, presumably activated hemocytes. (E–H) Antibody staining using the lamellocyte marker MAb L1b, reveals increases in lamellocyte number following *Pxn-GAL4*-mediated overexpression of *nej*, *Kr*, and *CG32813*. (I–L) Filamentous actin (F-actin) was revealed using rhodamine-phalloidin. (I) Weak F-actin staining is detected in plasmatocytes of the *Pxn-GAL4* driver line. Strong F-actin staining is detected in large hemocytes in (J) *Kr*-, (K) *nej*-, and (L) *CG32813*-overexpressing hemocytes, suggesting that these contain an actively polymerizing cytoskeleton network. (M–P) Antibody staining using antibodies against the Drosophila β-integrin Myospheroid (Mys) shows weak expression of Mys in control hemocytes (M), but strong expression in (N) *Kr*, (O) *nej*, and (P) *CG32813* overexpressing hemocytes. Upregulation of Mys was most apparent in hemocytes >15 μm. In A–P DNA (visualized using DAPI) is shown in white and antibody- and phalloidin-staining in green. Bar, 20 μm.

ton network, consistent with changes in their adherent properties.

As *Pxn-GAL4* is expressed at low levels in the larval fat body, the other principal immune-competent tissue, the possibility existed, albeit slight, that the hemocyte phenotypes observed above were triggered indirectly. Potentially, low-level misexpression of *Kr*, *nej*, or *CG32813* in the fat body may have disrupted the fat body, in turn eliciting a response in hemocytes. To exclude this possibility, we overexpressed *Kr*, *nej*, or *CG32813* exclusively in the fat body using the *Lsp2-GAL4* driver and found no change in any of the hemocyte properties examined (data not shown). This confirmed that *Pxn-GAL4* hemocyte phenotypes were cell autonomous.

Finally, we tested whether hemocytes were still functional after overexpression of either *Kr* or *nej*. Hemocytes in third instar larvae play a key role in innate immunity by phagocytosing foreign material. Normally this includes invading bacteria, but particles of India ink (a mixture of carbon particles of heterogeneous size) can also be recognized and engulfed by hemocytes. Forty minutes after injection of India ink into wandering-stage third instar larvae, particles of India ink can be detected in lysosomes in hemocytes of the parental *Pxn-GAL4/+* driver control (Figure 8A). Hemocytes that overexpressed *nej* were also able to engulf India ink particles, suggesting that they are still competent to engage in phagocytosis (Figure 8C). In contrast, hemocytes that overexpressed *Kr* did not engulf India ink particles. Instead hemocytes can be observed to adhere to larger particles of India ink (Figure 8B). It appeared that these cells had switched from a pathway in which small particles are engulfed to one in which larger particles are encapsulated.

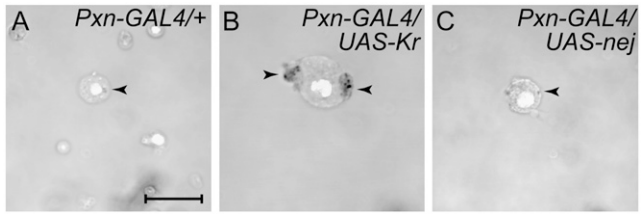

FIGURE 8.—Phagocytic properties of hemocytes. Hemocytes were isolated from wandering-stage third instar larvae 40 min after injection of India ink particles and visualized using phase contrast microscopy. (A) Small particles of India ink were detected in lysosomes (arrowhead) of hemocytes of the parental *Pxn-GAL4, UAS-GFP* driver indicating that phagocytosis was normal. (B) Larger hemocytes present after *Kr* overexpression did not engulf India ink particles but rather adhered to large particles of India ink (arrowheads). (C) Hemocytes overexpressing *nej* were still capable of engulfing India ink particles, detected in lysosomes (arrowhead). Bar, 20 μm.

This confirmed our earlier results in which we observed increased lamellocyte numbers in *Pxn-GAL4-xUAS-Kr* larvae. An encapsulation response is typical of lamellocytes and differentiation of lamellocytes is an important component of the innate immune response to larger pathogens such as parasitic wasp eggs. However, ectopic differentiation of lamellocytes also can lead to the inappropriate targeting and encapsulation of host tissue, leading to the production of inflammatory melanotic tumors. *Pxn-GAL4xUAS-Kr* larvae are viable and survive to the adult stage. However, ~40% of these flies exhibit melanotic tumors, consistent with deregulated lamellocyte function (data not shown).

DISCUSSION

In this study, we have conducted a misexpression screen to identify factors that regulate Drosophila larval hemocyte development and function. Using a hemocyte specific GAL4 driver, *Pxn-GAL4*, we screened 3412 EP and EY insertions and uncovered 108 insertions corresponding to 101 candidate genes that may be regulators of hemocyte development. This corresponds to a hit rate of 3.2% and compares favorably with recovery rates observed previously in gain-of-function screens in other tissues using EP elements. For example, 4.6% of EP insertions generate a phenotype when overexpressed in adult sensory organs (Abdelilah-Seyfried *et al.* 2000). Similarly, 1.5% of EP insertions screened affected muscle pattern formation (Staudt *et al.* 2005) and 9% of EP insertions screened generated a phenotype in the adult dorsal thorax (Pena-Rangel *et al.* 2002). We found that hit rates obtained using EP and EY lines were similar. Thus, 4% of EP lines screened affected hemocyte development while 3% of EY lines screened were positive.

As part of preparatory work for the screen we performed detailed characterization of the *Pxn-GAL4* driver at all larval instars, showing that it expresses in two Drosophila hemocyte lineages: plasmatocytes and crystal cells. This analysis also revealed that two distinct groups of plasmatocytes—a circulating and a sessile population—exist at all larval stages. The latter sessile hemocytes are distributed predominately at the posterior part of the larva and as segmentally repeated patches or compartments on the inner dorsal surface of the integument of most larval segments. These results are consistent with previous analyses of larval hemocytes that indicated the presence of sessile hemocyte islets (Lanot *et al.* 2001; Narita *et al.* 2004). However in this study we have been able to examine dynamics of these sessile hemocyte compartments and show they arise partly as a result of hemocyte recruitment from the circulating hemolymph, although cell division can also be detected within the sessile islets (data not shown). At this stage it is not obvious what features of the integument in these regions induce recruitment of hemocytes. It is clear, however, that these compartments are dynamic as hemocytes can be observed to detach from these regions, and they are disrupted in prepupal stages possibly as a result of rising ecdysone titers. Currently little is known about the function of these adherent hemocytes. One possibility is that these regions may simply act as a depot or reserve of hemocytes that can be liberated as required, either upon infection or at pupariation to take part in tissue remodeling. Alternatively they may provide a specialized function, for example, acting as sensors or sentinels for infections. Two hemocyte cell types, macrophages and crystal cells, can be detected in these regions, suggesting that both are responsive to cues from these regions. However, lamellocytes are not detected.

Taking advantage of the transparent nature of the Drosophila larval cuticle and by incorporating a *UAS-GFP* responder in the genetic background of the *Pxn-GAL4* driver line, we were able to screen for genes that affected the distribution of the sessile hemocyte compartment, altered hemocyte morphology and number, or which caused inappropriate targeting of hemocytes and changes in the lymph gland size. Among the observed phenotypes, disruption of the sessile dorsal hemocyte compartments was the most frequent category recorded. It is reasonable to expect that this phenotype is associated with defects in hemocyte adhesion properties, for example, altered production of cell adhesion molecules by hemocytes or changes in cytoskeleton organization in hemocytes. Consistent with this, we recovered insertions that misexpress *scb* (the Drosophila α-integrin αPS3), *C3G* (a Ras family guanine nucleotide exchange factor), and *RhoGEF2* within this category. In addition, we have been able to show that misexpression of *Kr*, *nej*, and *CG32813* led to elevated expression of the Drosophila β-integrin subunit Mys in hemocytes and that these hemocytes showed increased staining of F-actin using rhodamine-phalloidin, both consistent with changes in their adherent properties.

Enlargement of the larval lymph gland was the second most frequent phenotype observed. Given the similarities that have been proposed between lymph gland hematopoiesis in Drosophila and mammalian aorta-gonadal-mesonephros mesoderm development (Mandal *et al.* 2004), genes identified here may add important insights into developmental regulation of mammalian hematopoiesis. In principle, the lymph gland overgrowth phenotypes we recorded may have been caused by increases in hemocyte proliferation or by changes in hemocyte survival. Banerjee and co-workers (Jung *et al.* 2005) have shown that proliferation in the third larval instar lymph gland is restricted to the cortical zone. Importantly, expression of *Pxn-GAL4* in the lymph gland is limited to mature hemocytes also located in the cortical zone. As such, factors recovered in this screen are likely to regulate

the expansion phase of lymph gland development, when mature hemocytes divide to increase numbers. One factor that we have identified with an enlarged lymph gland phenotype is the microRNA *bantam*, which has been shown to control both proliferation and apoptosis (Brennecke *et al.* 2003) and which is a target of the Hippo pathway (Nolo *et al.* 2006; Thompson and Cohen 2006). Interestingly misexpression of two histone demethylases, the histone H3K9 demethylase *CG33182* (also known as JMJD2C) and the Drosophila Jumonji homolog *CG3654*, also gave a lymph gland overgrowth phenotype. In humans JMJD2C has been found to be amplified in cell lines derived from esophageal squamous carcinomas while knockdown of JMJD2C leads to decreased cell proliferation (Cloos *et al.* 2006).

A GAL4 screen for regulators of larval hemocyte function has identified a number of critical signaling pathways that regulate hemocyte activation (Zettervall *et al.* 2004). However, this screen was a directed screen that altered function of a set of 33 genes that were predicted to affect hemocyte development. In this report we have substantially extended this work by screening ~20% of Drosophila genes. Moreover, our screen has been performed using the *Pxn-GAL4* driver that expresses in mature plasmatocytes. This has allowed us to recover regulators of mature plasmatocyte adhesion and function without the complication of altering plasmatocyte determination by expression of these factors at earlier stages in the hemocyte lineage.

A final caveat that must be considered is that a proportion of the genes recovered in misexpression screens may not necessarily be normally expressed or function within the tissue assayed. As such, some of the candidate genes identified here may not have a normal function in hemocyte development. Moreover, a number of the genes identified appear to be general factors involved in cell development and are not hemocyte specific. To confirm which genes are *bona fide* regulators of hemocyte function it will be necessary to determine expression profile and loss-of-function phenotypes of these genes. Increasing availability of inducible RNAi lines (Kambris *et al.* 2006; Dietzl *et al.* 2007) will make this an important future avenue of research.

We thank I. Ando, M. Galko, D. Hultmark, R. Hynes, H. Jäckle, J. Kumar, and L. Waltzer for generously providing flies and reagents. EP and EY transposons used in this screen were kindly provided by the Bloomington and Szeged Drosophila Stock Centers. We thank C. Buckley, and M. Mortin for critical reading of the manuscript and M. Krajcovic for assistance preparing fly food. This work was partly supported by grants from the Royal Society, the Rowbotham Bequest, and the Medical Research Council (United Kingdom).

LITERATURE CITED

Abdelilah-Seyfried, S., Y. M. Chan, C. Zeng, N. J. Justice, S. Younger-Shepherd *et al.*, 2000 A gain-of-function screen for genes that affect the development of the Drosophila adult external sensory organ. Genetics **155:** 733–752.

Abrams, J. M., K. White, L. I. Fessler and H. Steller, 1993 Programmed cell death during Drosophila embryogenesis. Development **117:** 29–43.

Alfonso, T. B., and B. W. Jones, 2002 gcm2 promotes glial cell differentiation and is required with glial cells missing for macrophage development in Drosophila. Dev. Biol. **248:** 369–383.

Baker, N. E., and A. E. Zitron, 1995 Drosophila eye development: Notch and Delta amplify a neurogenic pattern conferred on the morphogenetic furrow by scabrous. Mech. Dev. **49:** 173–189.

Barrett, K., M. Leptin and J. Settleman, 1997 The Rho GTPase and a putative RhoGEF mediate a signaling pathway for the cell shape changes in Drosophila gastrulation. Cell **91:** 905–915.

Bataille, L., B. Auge, G. Ferjoux, M. Haenlin and L. Waltzer, 2005 Resolving embryonic blood cell fate choice in Drosophila: interplay of GCM and RUNX factors. Development **132:** 4635–4644.

Bellen, H. J., R. W. Levis, G. Liao, Y. He, J. W. Carlson *et al.*, 2004 The BDGP gene disruption project: single transposon insertions associated with 40% of Drosophila genes. Genetics **167:** 761–781.

Bernardoni, R., V. Vivancos and A. Giangrande, 1997 glide/gcm is expressed and required in the scavenger cell lineage. Dev. Biol. **191:** 118–130.

Brand, A. H., and N. Perrimon, 1993 Targeted gene expression as a means of altering cell fates and generating dominant phenotypes. Development **118:** 401–415.

Brennecke, J., D. R. Hipfner, A. Stark, R. B. Russell and S. M. Cohen, 2003 bantam encodes a developmentally regulated microRNA that controls cell proliferation and regulates the proapoptotic gene hid in Drosophila. Cell **113:** 25–36.

Brogiolo, W., H. Stocker, T. Ikeya, F. Rintelen, R. Fernandez *et al.*, 2001 An evolutionarily conserved function of the Drosophila insulin receptor and insulin-like peptides in growth control. Curr. Biol. **11:** 213–221.

Carrera, P., S. Abrell, B. Kerber, U. Walldorf, A. Preiss *et al.*, 1998 A modifier screen in the eye reveals control genes for Kruppel activity in the Drosophila embryo. Proc. Natl. Acad. Sci. USA **95:** 10779–10784.

Cloos, P. A., J. Christensen, K. Agger, A. Maiolica, J. Rappsilber *et al.*, 2006 The putative oncogene GASC1 demethylates tri- and dimethylated lysine 9 on histone H3. Nature **442:** 307–311.

Crozatier, M., J. M. Ubeda, A. Vincent and M. Meister, 2004 Cellular immune response to parasitization in Drosophila requires the EBF orthologue collier. PLoS Biol. **2:** E196.

Delaunay, J., G. Le Mee, N. Ezzeddine, G. Labesse, C. Terzian *et al.*, 2004 The Drosophila Bruno paralogue Bru-3 specifically binds the EDEN translational repression element. Nucleic Acids Res. **32:** 3070–3082.

Dietzl, G., D. Chen, F. Schnorrer, K. C. Su, Y. Barinova *et al.*, 2007 A genome-wide transgenic RNAi library for conditional gene inactivation in Drosophila. Nature **448:** 151–156.

Escudero, L. M., E. Caminero, K. L. Schulze, H. J. Bellen and J. Modolell, 2005 Charlatan, a Zn-finger transcription factor, establishes a novel level of regulation of the proneural achaete/scute genes of Drosophila. Development **132:** 1211–1222.

Evans, C. J., V. Hartenstein and U. Banerjee, 2003 Thicker than blood: conserved mechanisms in Drosophila and vertebrate hematopoiesis. Dev. Cell **5:** 673–690.

Fujimoto, K., N. Okino, S. Kawabata, S. Iwanaga and E. Ohnishi, 1995 Nucleotide sequence of the cDNA encoding the proenzyme of phenol oxidase A1 of Drosophila melanogaster. Proc. Natl. Acad. Sci. USA **92:** 7769–7773.

Gregory, S. L., T. Shandala, L. O'Keefe, L. Jones, M. J. Murray *et al.*, 2007 Drosophila overexpression screen for modifiers of Rho signalling in cytokinesis. Fly **1:** 13–22.

Hacker, U., and N. Perrimon, 1998 DRhoGEF2 encodes a member of the Dbl family of oncogenes and controls cell shape changes during gastrulation in Drosophila. Genes Dev. **12:** 274–284.

Holz, A., B. Bossinger, T. Strasser, W. Janning and R. Klapper, 2003 The two origins of hemocytes in Drosophila. Development **130:** 4955–4962.

Ishimaru, S., R. Williams, E. Clark, H. Hanafusa and U. Gaul, 1999 Activation of the Drosophila C3G leads to cell fate changes and overproliferation during development, mediated by the RAS-MAPK pathway and RAP1. EMBO J. **18:** 145–155.

Jia, S., and A. Meng, 2007 Tob genes in development and homeostasis. Dev. Dyn. **236:** 913–921.

Jones, S. L., F. P. Lindberg and E. J. Brown, 1999 *Phagocytosis*. J. B. Lippincott, Philadelphia.

Jung, S. H., C. J. Evans, C. Uemura and U. Banerjee, 2005 The Drosophila lymph gland as a developmental model of hematopoiesis. Development **132:** 2521–2533.

Kambris, Z., S. Brun, I. H. Jang, H. J. Nam, Y. Romeo *et al.*, 2006 Drosophila immunity: a large-scale in vivo RNAi screen identifies five serine proteases required for Toll activation. Curr. Biol. **16:** 808–813.

Kumar, J. P., T. Jamal, A. Doetsch, F. R. Turner and J. B. Duffy, 2004 CREB binding protein functions during successive stages of eye development in Drosophila. Genetics **168:** 877–893.

Kurucz, E., C. J. Zettervall, R. Sinka, P. Vilmos, A. Pivarcsi *et al.*, 2003 Hemese, a hemocyte-specific transmembrane protein, affects the cellular immune response in Drosophila. Proc. Natl. Acad. Sci. USA **100:** 2622–2627.

Lai-Fook, J., 1966 The repair of wounds in the integument of insects. J. Insect Physiol. **12:** 195–226.

Lanot, R., D. Zachary, F. Holder and M. Meister, 2001 Postembryonic hematopoiesis in Drosophila. Dev. Biol. **230:** 243–257.

Lebestky, T., T. Chang, V. Hartenstein and U. Banerjee, 2000 Specification of Drosophila hematopoietic lineage by conserved transcription factors. Science **288:** 146–149.

Long, H., S. Cameron, L. Yu and Y. Rao, 2006 De novo GMP synthesis is required for axon guidance in Drosophila. Genetics **172:** 1633–1642.

Luo, H., W. P. Hanratty and C. R. Dearolf, 1995 An amino acid substitution in the Drosophila hopTum-l Jak kinase causes leukemia-like hematopoietic defects. EMBO J. **14:** 1412–1420.

Mandal, L., U. Banerjee and V. Hartenstein, 2004 Evidence for a fruit fly hemangioblast and similarities between lymph-gland hematopoiesis in fruit fly and mammal aorta-gonadal-mesonephros mesoderm. Nat. Genet. **36:** 1019–1023.

Manseau, L., A. Baradaran, D. Brower, A. Budhu, F. Elefant *et al.*, 1997 GAL4 enhancer traps expressed in the embryo, larval brain, imaginal discs, and ovary of Drosophila. Dev. Dyn. **209:** 310–322.

Maroni, G., and S. C. Stamey, 1983 Use of blue food to select synchronous, late third-instar larvae. Dros. Inf. Serv. **59:** 142–143.

Meister, M., and M. Lagueux, 2003 Drosophila blood cells. Cell. Microbiol. **5:** 573–580.

Mukherjee, T., U. Schafer and M. P. Zeidler, 2006 Identification of Drosophila genes modulating janus kinase/signal transducer and activator of transcription signal transduction. Genetics **172:** 1683–1697.

Narita, R., H. Yamashita, A. Goto, H. Imai, S. Ichihara *et al.*, 2004 Syndecan-dependent binding of Drosophila hemocytes to laminin alpha3/5 chain LG4–5 modules: potential role in sessile hemocyte islets formation. FEBS Lett. **576:** 127–132.

Nolo, R., C. M. Morrison, C. Tao, X. Zhang and G. Halder, 2006 The bantam microRNA is a target of the hippo tumor-suppressor pathway. Curr. Biol. **16:** 1895–1904.

Pena-Rangel, M. T., I. Rodriguez and J. R. Riesgo-Escovar, 2002 A misexpression study examining dorsal thorax formation in *Drosophila melanogaster*. Genetics **160:** 1035–1050.

Ramet, M., P. Manfruelli, A. Pearson, B. Mathey-Prevot and R. A. Ezekowitz, 2002 Functional genomic analysis of phagocytosis and identification of a Drosophila receptor for E. coli. Nature **416:** 644–648.

Rehorn, K. P., H. Thelen, A. M. Michelson and R. Reuter, 1996 A molecular aspect of hematopoiesis and endoderm development common to vertebrates and Drosophila. Development **122:** 4023–4031.

Rorth, P., 1996 A modular misexpression screen in Drosophila detecting tissue-specific phenotypes. Proc. Natl. Acad. Sci. USA **93:** 12418–12422.

Ruiz-Gomez, M., S. Romani, C. Hartmann, H. Jackle and M. Bate, 1997 Specific muscle identities are regulated by Kruppel during Drosophila embryogenesis. Development **124:** 3407–3414.

Sinenko, S. A., E. K. Kim, R. Wynn, P. Manfruelli, I. Ando *et al.*, 2004 Yantar, a conserved arginine-rich protein is involved in Drosophila hemocyte development. Dev. Biol. **273:** 48–62.

Soderhall, K., and L. Cerenius, 1998 Role of the prophenoloxidase-activating system in invertebrate immunity. Curr. Opin. Immunol. **10:** 23–28.

Sorrentino, R. P., Y. Carton and S. Govind, 2002 Cellular immune response to parasite infection in the Drosophila lymph gland is developmentally regulated. Dev. Biol. **243:** 65–80.

Staudt, N., A. Molitor, K. Somogyi, J. Mata, S. Curado *et al.*, 2005 Gain-of-function screen for genes that affect Drosophila muscle pattern formation. PLoS Genet. **1:** e55.

Stramer, B., W. Wood, M. J. Galko, M. J. Redd, A. Jacinto *et al.*, 2005 Live imaging of wound inflammation in Drosophila embryos reveals key roles for small GTPases during in vivo cell migration. J. Cell Biol. **168:** 567–573.

Tanaka-Matakatsu, M., T. Uemura, H. Oda, M. Takeichi and S. Hayashi, 1996 Cadherin-mediated cell adhesion and cell motility in Drosophila trachea regulated by the transcription factor Escargot. Development **122:** 3697–3705.

Tepass, U., L. I. Fessler, A. Aziz and V. Hartenstein, 1994 Embryonic origin of hemocytes and their relationship to cell death in Drosophila. Development **120:** 1829–1837.

Thompson, B. J., and S. M. Cohen, 2006 The Hippo pathway regulates the bantam microRNA to control cell proliferation and apoptosis in Drosophila. Cell **126:** 767–774.

Tsuda, L., M. Kaido, Y. M. Lim, K. Kato, T. Aigaki *et al.*, 2006 An NRSF/REST-like repressor downstream of Ebi/SMRTER/Su(H) regulates eye development in Drosophila. EMBO J. **25:** 3191–3202.

Wang, X., C. Lee, D. S. Gilmour and J. P. Gergen, 2007 Transcription elongation controls cell fate specification in the Drosophila embryo. Genes Dev. **21:** 1031–1036.

Williams, M. J., M. L. Wiklund, S. Wikman and D. Hultmark, 2006 Rac1 signalling in the Drosophila larval cellular immune response. J. Cell Sci. **119:** 2015–2024.

Wood, W., C. Faria and A. Jacinto, 2006 Distinct mechanisms regulate hemocyte chemotaxis during development and wound healing in Drosophila melanogaster. J. Cell Biol. **173:** 405–416.

Yamaguchi, Y., T. Takagi, T. Wada, K. Yano, A. Furuya *et al.*, 1999 NELF, a multisubunit complex containing RD, cooperates with DSIF to repress RNA polymerase II elongation. Cell **97:** 41–51.

Yee, G., and R. O. Hynes, 1993 A novel, tissue-specific integrin subunit, beta nu, expressed in the midgut of Drosophila melanogaster. Development **118:** 845–858.

Yuan, J., W. Tang, K. Luo, X. Chen, X. Gu *et al.*, 2006 Cloning and characterization of the human gene DERP6, which activates transcriptional activities of p53. Mol. Biol. Rep. **33:** 151–158.

Zettervall, C. J., I. Anderl, M. J. Williams, R. Palmer, E. Kurucz *et al.*, 2004 A directed screen for genes involved in Drosophila blood cell activation. Proc. Natl. Acad. Sci. USA **101:** 14192–14197.

Communicating editor: J. A. Lopez